NASA TECHNICAL NOTE

NASA TN D-7788

NASA TN D-7788

SOME OBSERVATIONS ABOUT THE COMPONENTS OF TRANSONIC FAN NOISE FROM NARROW-BAND SPECTRAL ANALYSIS

by Arthur V. Saule

Lewis Research Center
Cleveland, Ohio 44135

NATIONAL AERONAUTICS AND SPACE ADMINISTRATION • WASHINGTON, D. C. • OCTOBER 1974

SOME OBSERVATIONS ABOUT THE COMPONENTS OF TRANSONIC FAN NOISE FROM NARROW-BAND SPECTRAL ANALYSIS

by Arthur V. Saule

Lewis Research Center

SUMMARY

Qualitative and quantitative spectral analyses are presented that give the broadband-noise, discrete-tone, and multiple-tone properties of the noise generated by a full-scale high-bypass single-stage axial-flow transonic fan (fan B, NASA Quiet Engine Program). The noise components were obtained from narrow-band spectra in conjunction with 1/3-octave-band spectra. Variations in the pressure levels of the noise components with fan speed, forward-quadrant azimuth angle, and frequency are presented and compared. The study shows that much of the apparent broadband noise on 1/3-octave-band plots consists of a complex system of shaft-order tones. The analyses also indicate the difficulties in determining or defining noise components, especially the broadband level under the discrete tones. The sources which may be associated with the noise components are indicated and discussed.

INTRODUCTION

The dominant noise source in high-bypass turbofan engines is the fan stage, and considerable experimental and theoretical research has been devoted to understanding the nature of this noise source and finding ways to reduce its output (e.g., refs. 1 to 5). The fan noise spectral analysis has proved to be a powerful experimental measurement in studying this noise. From an analysis of their spectra, the components of fan noise can be identified as discrete tones, broadband noise, and multiple tones. The spectral analyses are an important link with the theoretical studies which provide models or mechanisms that describe the generation of these characteristic fan noises.

Much of the published data (e.g., ref. 2) consists of 1/3-octave-band spectral analysis. While the degree of resolution provided by this analysis is satisfactory for some purposes, it does not give sufficient resolution to allow precise identification

and quantification of the noise components. This problem has been recognized for some time, but, for many reasons, narrow-band analyses, which would provide better spectral resolution, are not routinely performed.

This report first presents some preliminary qualitative observations about the noise signature and nature of the source from a full-scale transonic design fan as noted from narrow-band spectra of the far-field data. Then a quantitative spectral component analysis routine based upon these observations is presented for evaluating broadband-noise, discrete-tone, and multiple-tone acoustic pressure levels. These noise components are obtained interdependently from 1/3-octave-band and narrow-band spectra. The experimental observations are presented and discussed in relation to noise generation theories and mechanisms.

The data presented are for fan B of the NASA Quiet Engine Program (ref. 2) as tested in the Lewis full-scale fan facility (ref. 5). The data are for far-field measurements taken at 10° intervals along a 30.5-meter-radius arc of the fan. The fan tip speed was varied from 60 to 90 percent of the design value of 354 meters per second. The results show the behavior of the noise components of this fan stage with tip speed and with changes in angular position in the forward quadrant from 10° to 90° measured from the fan inlet axis.

Although the data analysis routine has been developed from fan B acoustic measurements, it is not restricted to this particular fan. On the other hand, the numerical findings and conclusions discussed in this report are based solely on transonic fan B noise data and may not represent the acoustic performance of other high-bypass fans of similar configuration.

TEST APPARATUS

Facility

Figure 1 shows a plan view of the full-scale-fan acoustic test facility located at the NASA Lewis Research Center. The test fan was positioned some distance from the wall of the main drive building with the exhaust nozzle facing the free field.

Far-field acoustic measurements of the test fan were made by using 16 microphones mounted on poles at the elevation of the fan axis, 5.8 meters above the grade level. All microphones were located in the same horizontal plane on 30.5-meter radii with the origin near the exhaust plane of the fan bypass nozzle. A more detailed description of the apparatus and the instrumentation is given in the appendix and reference 5.

Fan Design Characteristics

Fan B was designed and built as part of the NASA Quiet Engine Program. One of the objectives of this program was the application of the current state of the art to the development of low-noise turbofans. Low-noise features incorporated in the fan B design were (1) absence of inlet guide vanes, (2) use of a single rotor-stator stage, (3) extended rotor-stator spacing, (4) selection of the number of rotor blades and their angular design speed to cause fundamental tones to appear in frequency bands of low annoyance level, and (5) use of a vane-blade number ratio in excess of 2 to reduce the magnitude of the fundamental tone due to rotor-stator interaction. In addition, the particular configuration considered in this analysis had fan frame acoustic treatment and core duct noise suppression. This configuration is illustrated in figure 2, which shows the arrangement of the flow passages and general design features.

The rotor of fan B had 26 aluminum low-aspect-ratio twisted blades without vibration dampers. The bypass duct stator had 60 vanes; the core duct stator had 60 forward and 60 aft vanes arranged in tandem. The number of rotor chords axially separating the rotor and stators was 2 in the bypass duct and 1.25 in the core duct.

The fan is an axial-flow air compressor 1.86 meters in diameter designed to deliver a bypass total-pressure ratio of 1.5 at a total flow rate of 431 kilograms per second, 87 percent efficiency, and an angular design speed of 3625 rpm (tip speed of 354 m/sec). The design rotor tip circumferential Mach number is 1.07; the flow relative to the rotor tip has a Mach number of 1.2. The corresponding Mach numbers at the hub station in the rotor inlet plane are 0.5 and 0.8, respectively. The approximate Mach numbers at test speeds can be obtained by multiplying the design values by percent of design speed. Further discussions of the fan design and configuration are given in references 2, 6, and 7.

DATA REDUCTION

The acoustic testing of fan B was done at the NASA Lewis Research Center. Altogether three separate sets of acoustic data were taken at each speed at each of 16 microphone locations. Data at 60 and 90 percent design speed were utilized for the present study. The fan was not run at 100 percent design speed.

Each acoustic recording was 100 seconds in duration and yielded a 1/3-octave-band analysis covering frequency bands with center frequencies from 50 to 20 000 hertz. The test-day sound pressure levels of three sample runs were arithmetically averaged to minimize the effect of random variations. In addition, a similar set of 1/3-octave-band data was computed by removing the effect of atmospheric absorption from the

test-day data (ref. 4). The adjusted data were thus referred back to the source and are called referred sound pressure levels.

Continuous narrow-band spectral analyses of the noise signals were also performed. In general, this analysis system employed a 20-hertz nominal bandwidth filter. In this report the bandwidth is identified by its nominal value. For quantitative evaluation, however, the equivalent or effective bandwidths were used; they were obtained by multiplying the nominal value by 1.6. The 20-hertz-bandwidth analysis together with 1/3-octave-band spectra provided the numerical data for a quantitative evaluation of sound pressure levels of the noise components, which is discussed in the next section. Narrow-band analyses with higher than 20-hertz-bandwidth resolution were limited to the 40° azimuth angle and were used for a qualitative comparison only. Since all the narrow-band spectra reflect the signals under test-day conditions, the sound pressure levels obtained from the narrow-band spectra were adjusted for atmospheric attenuation of the test day, averaged, and converted to 1/3-octave-band referred levels for each frequency band. Only data for bands with center frequencies from 400 to 8000 hertz were used in this study because this frequency range covered the major noise features of fan B.

SPECTRAL COMPONENT ANALYSIS

The following component analysis determines the pressure levels of fan discrete tones, broadband noise, and multiple tones. In this report, the tones which appear at blade passing frequency and their harmonics are defined as discrete tones. Random acoustic signals with spectra whose extent in the frequency domain is broad, compared with the analysis bandwidth, are called broadband noise. The tones which occur at shaft rotating frequencies and their multiples (excluding blade passing frequency and its harmonics) are called multiple tones.

Spectral Characteristics of Test Fan

A qualitative spectral investigation of the acoustic data of fan B has been undertaken in this section to examine those spectral features which may affect the quantitative evaluation of the noise components. The qualitative analysis is also used in recognizing and more precisely defining the various spectral components from intricate noise signatures. Furthermore, it serves to establish the guidelines for the subsequent quantitative evaluation of the noise components. For this purpose, 1/3-octave-band as well as narrow-band spectra are utilized.

1/3-Octave-band spectrum. - The spectral characteristics of fan B, described by a conventional 1/3-octave-band spectrum, are illustrated in figure 3(a). The spectrum represents test-day data of one of the three sample runs of the fan at 90 percent speed and a 40° azimuth angle over a center frequency range from 50 to 20 000 hertz. The bands with center frequencies from 400 to 8000 hertz are numbered from 10 to 23. The band limits are delineated by vertical dashed lines.

The 1/3-octave-band spectrum is seen to be characterized by a relatively smooth transition from one band to another from approximately 80 to 1000 hertz and above 5000 hertz. The exception is between 1000 and 5000 hertz, where five data points protrude above the rest of the spectrum by approximately 4 to 15 decibels. The data points in bands 15, 18, and 20 are associated with the fundamental tone at blade passing frequency (1392 Hz) and its second and third harmonics at 2784 and 4176 hertz, respectively. The other two data points in bands 16 and 19 can be identified with band splitting of the fundamental tone and its second harmonic, respectively.

Thus, it appears from the figure that the discrete tones were superimposed on some broadband base anchored at the data points in bands 14, 17, and 21. Such a concept of a two-component composition of the fan noise is consistent with the earlier subsonic fan noise theories as advanced, for example, by Sharland (ref. 8), Smith and House (ref. 9), and Richards and Mead (ref. 10) from their studies of similar 1/3-octave-band data.

The theory of two-component spectra leads to a relatively straightforward evaluation of the spectral components: they are broadband noise and discrete tones, from which the broadband level underneath the five data points is arbitrarily established by connecting the given anchor points by straight lines (long and short dashes). As shown in figure 3(a), the straight line approximation gives a relatively good fit to the rest of the continuous spectrum. In this report the broadband-noise and discrete-tone pressure levels obtained from the 1/3-octave-band spectrum are called apparent levels to distinguish them from similar component levels determined from the following narrow-band analysis and designated as the actual baseline in figure 3(a) by the long-dash curve.

Twenty-hertz-bandwidth spectrum. - A 20-hertz-bandwidth spectrum over the frequency range from 0 to 10 000 hertz is shown in figure 3(b) for the same sample run as in figure 3(a). Compared with 1/3-octave-band analysis, the 20-hertz-bandwidth spectrum reveals several marked differences.

The 20-hertz-bandwidth spectrum is characterized by closely spaced noise clusters, prominently displayed all over the spectrum. The noise clusters appear in the frequency range just below the fundamental tone and between the discrete-tone harmonics at seemingly regular intervals. Closer inspection of a typical cluster, for example, that in band 17, indicates that the clusters may contain a spectral

structure similar to a line spectrum. However, it is evident that higher resolution details are required to resolve definitely the nature of the clusters.

Another characteristic of the 20-hertz-bandwidth spectrum is the broadening of discrete tones. The broadening spreads from the peak down in a skirtlike fashion and terminates at relatively widely separated minimums. Otherwise, the discrete-tone "skirts" on the 20-hertz-bandwidth spectrum do not seem to indicate any periodic features similar to the clusters.

It is seen from figure 3(b) that the bands containing the straight line portion of the apparent broadband pressure level discussed in the previous section (bands 14 to 21, fig. 3(a)) contain most of the prominent clusters and skirts. The actual baseline shown in figure 3(b) was arbitrarily established by connecting the minimums of the spectrum by a continuous (long-dash) curve; this procedure is discussed in more detail in the next section, which describes a quantitative evaluation of the spectral components. Figure 3(b) also shows that the 20-hertz-bandwidth analysis does not offer conclusive evidence to alter the two-component concept or the levels of the spectral components established by the 1/3-octave-band analysis. Nevertheless, the extent and the nature of the clusters and skirts suggest a need for still higher resolution spectra.

Higher resolution spectra. - The sample run used in figure 3(b) is shown in figure 3(c), resolved into a 10-hertz-bandwidth spectrum. The figure indicates that the clusters first noticed on the 20-hertz-bandwidth spectrum as closely spaced protrusions can now be clearly identified as shaft-order tones, repeating at intervals of shaft rotating frequency. Also, the tones in the clusters are not equal in magnitude and show a tendency toward a maximum about a central tone which seems to occur at multiples of one-half of the blade passage frequency, 696 hertz.

Figure 3(c) also shows that all shaft-order tones can be identified, although a definite count of the tones in each cluster is complicated by the adjacent discrete-tone skirts. Examination of the skirts reveals that they do not fall uniformly toward the broadband base, as was indicated by the 20-hertz-bandwidth spectra. Instead, the skirts exhibit distinct periodic protrusions which also repeat at the intervals of shaft rotating frequency.

The clusterlike structure of the discrete tones is resolved into even finer detail in figure 3(d), a 4-hertz-bandwidth spectrum from 0 to 2000 hertz. The figure shows the skirt protrusions around the fundamental tone as distinct shaft-order tones numbered from 22 to 30, where the 26th shaft-order tone is also the fundamental discrete tone. The 4-hertz-bandwidth spectrum also shows that several shaft-order tones exhibit sidebands, which are tones formed immediately outside the assigned bands of shaft-order tones. However, the magnitudes of these sidebands are relatively small. In this report, the shaft-order tones and their sidebands are called multiple tones.

Summary of basic components. - The previous step-by-step qualitative analysis shows the basic spectral components of an initially relatively crude 1/3-octave-band spectrum (fig. 3(a)). This analysis provides the groundwork for the quantitative description given in the next section. Figure 3(a) illustrates the conventional 1/3-octave-band two-component spectral distribution of sound pressure level, where the discrete tones are superimposed on an apparent broadband base. A 20-hertz-bandwidth spectrum (fig. 3(b)) discloses the existence of clusters and discrete-tone skirts. Signs of possible periodic signals in the clusters suggest the need for spectra of still higher resolution. A 10-hertz-bandwidth spectrum (fig. 3(c)) shows that the clusters are composed of a series of shaft-order tones. Further investigation of the clusters on a 4-hertz-bandwidth spectrum (fig. 3(d)) reveals sidebands of the shaft-order tones.

The major results of this qualitative analysis of fan B noise spectra are indicated by a model spectra in figure 4, where the observed spectrum is pictured as an idealized synthesis of multiple tones (fig. 4(a)), discrete tones (fig. 4(b)), and broadband noise. The superposition of these components results in the complete spectrum shown in figure 4(c). In the model of figure 4(c), it is recognized that the broadband base may not necessarily be "linear," especially under the discrete tones, where broadband humps may be present instead of a straight-line interpretation.

Quantitative Evaluation of Spectral Components

In this section, the actual determination of the sound pressure levels of broadband noise, discrete tones, and multiple tones is performed by an interdependent use of 1/3-octave-band and 20-hertz-bandwidth spectra. For this purpose, the examples discussed in the preceding sections are again used.

Broadband noise. - Methods for evaluating broadband sound pressure level of aircraft engine fan noise have been reported previously (e.g., refs. 9 and 11 to 13). Many of these methods established the broadband level from the analysis of 1/3-octave-band spectra. For example, in the study of reference 11 the broadband noise level was established on a 1/3-octave-band spectrum by fairing in a curve underneath the discrete tones and the maximums of subharmonic tones (representing groups of shaft-order tones) which existed in the fan spectra considered in that reference. The discrete-tone and maximum levels of shaft-order tones were then subtracted from the overall sound pressure level. The remainder was designated as the broadband-noise pressure level.

The procedure in this report differs from the method of reference 11 in that it graphically establishes the broadband-noise baseline exclusively from a 20-hertz-bandwidth spectrum after a rather systematic qualitative investigation of a series of higher resolution spectra. This more involved route of probing consistently into higher resolution spectra indicated that 1/3-octave-band spectra may not be adequate

for determining the broadband-noise base for this particular fan because of the presence of multiple tones over the entire frequency spectrum and for all speeds tested.

The previous experience with higher resolution spectra suggested that multiple tones in the clusters and skirts must, like discrete tones, be superimposed on some broad continuous spectral substratum. When this idea is adapted from the two-component concept, the multiple tone substratum is established as the broadband noise. A baseline representing such a substratum is shown in figure 3(b) by a long-dash curve to indicate this interpretation.

As shown in figure 3(b), the broadband baseline is, in general, continuous and touches most of the minimums of the spectra, as implied by higher resolution spectra, except underneath the discrete tones. It is obvious that this interpretation allows definition of the broadband noise without including any line spectra or tone content that might be present but unidentified in 1/3-octave-band spectra. But it is also evident, for example, from the spectra shown in figures 3(c) and (d) that this interpretation of broadband noise may be uncertain underneath the discrete-tone skirts and could be improved if the behavior of the broadband noise in these regions is known. However, even a straight line approximation of the broadband noise established from narrow-band analysis (fig. 3(b)) appears to be already a definite improvement when it is compared with a similar interpretation based on a 1/3-octave-band spectrum (fig. 3(a)). The range of uncertainty of the broadband base underneath the fundamental tone on the 1/3-octave-band spectrum extends over approximately 1000 hertz; it is only approximately 500 hertz wide on the 4-hertz-bandwidth spectrum. Nevertheless, as shown in figures 3(b), (c), and (d), there is a possibility that the broadband level is underrated and the magnitude of discrete and multiple tones is overrated for the frequency regions covered by the discrete-tone skirts.

Since the actual narrow-band continuous spectrum level cannot exceed the apparent broadband level as a limit, the levels from the 20-hertz-bandwidth spectrum shown in figure 3(b) were checked for consistency with the apparent broadband-noise levels given in figure 3(a) on the basis of the 1/3-octave band. To aid the conversion, the frequency range of interest in the 20-hertz-bandwidth spectrum (400 to 8000 Hz) was divided into 14 divisions. In figure 3(b), these divisions are drawn as rectangular columns separated by vertical dashed lines which are made to coincide with the respective 1/3-octave-band frequency limits. The vertical extent of each rectangular column is terminated at the point where the indicated broadband-noise baseline meets the geometric center at the top of the column. The readings of sound pressure levels at these locations were assumed to be associated with the average sound pressure in the corresponding 1/3-octave band. The conversion from the 20-hertz-band level to the 1/3-octave-band level was accomplished in the usual way by adding to the 20-hertz-band level 10 times the

logarithm of the ratio of the respective 1/3-octave bandwidth to the 20-hertz effective bandwidth, taken to be approximately equal to 32 hertz (e.g., refs. 14 to 16).

When the sound pressure levels of more complex noise spectra than that shown in figure 3(b) were evaluated, it was more convenient first to convert the 20-hertz-bandwidth broadband level to broadband spectrum levels. The corresponding 1/3-octave-band levels were then determined by adding to the spectrum level 10 times the logarithm of the 1/3-octave bandwidth. The spectrum level is defined as the average sound pressure level in decibels referred to a band 1 hertz wide.

When the broadband noise was estimated, no attempt was made to achieve a perfect match between the calculated 20-hertz-bandwidth levels and the given 1/3-octave-band levels. It was observed that two noise spectra obtained from the same tape seldom had exactly the same signature, principally because the acoustic recordings (each 100 sec in duration) also varied somewhat from one portion of the magnetic tape to another as a result of short-term fluctuations. Since the end product was an average 1/3-octave-band sound pressure, three sample runs of 20-hertz-bandwidth data were used to obtain the average level, and thus random variations were minimized. Referred broadband-noise data were determined by correcting the test-day data for atmospheric absorption.

Discrete tones. - The 20-hertz-bandwidth spectra are also utilized for determining the discrete-tone levels. As shown in figure 3(b), all harmonically related tones can be clearly displayed within the given frequency range. On the other hand, 1/3-octave-band spectra, which are occasionally used to determine the discrete-tone content (e.g., ref. 11), reveal only the most prominent tones, and they are often complicated by band splitting, as shown in figure 3(a). For a 20-hertz-bandwidth spectrum, discrete-tone pressure levels are readily calculated from the established baseline broadband level (as in fig. 3(b)) and the maximum levels of the blade passing frequency harmonics. The discrete-tone levels obtained from the 20-hertz-bandwidth spectra are directly comparable with the corresponding 1/3-octave-band broadband levels without conversion because the tone levels remain the same irrespective of the bandwidth. The only correction required is for atmospheric attenuation to establish the referred discrete-tone pressure level.

Because of the multiple tones in the discrete-tone skirts (e.g., fig. 3(d)), the tonal content of the skirts at the frequencies other than multiples of the blade passing frequency was determined in the same manner as the multiple tones discussed in the next section. This routine is also consistent with the basic definition of the discrete tone as a single-frequency noise component.

Multiple tones. - Theoretically, the pressure levels of the multiple tones may be obtained in the same way as the levels of the discrete tones. The height of each multiple tone could be measured above the broadband level. The multiple-tone level then can be

obtained from known quantities by using conventional decibel algebra. This procedure, however, would require a continuous use of high-resolution spectra in which the multiple tones and their bases can be clearly distinguished in the clusters and discrete-tone skirts. Since such a direct way of obtaining multiple-tone levels is time consuming, for the purpose of this report, an indirect approach was more convenient. Graphically, the actual broadband level as established from the narrow-band data (e.g., fig. 3(b)) and adjusted to the 1/3-octave-band sound pressure level (fig. 3(a)) was first logarithmically added to the discrete-tone level as determined from the narrow-band data. The sum was then logarithmically subtracted from the overall sound pressure level from the 1/3-octave-band analysis as defined in the next section. The remainder was designated as the multiple-tone pressure level.

Calculation procedure. - In summary, the essential steps of the quantitative evaluation of the fan noise spectral components are as follows:

(1) Establish graphically the broadband-noise baseline on 20-hertz-bandwidth spectra at the spectral minimums.

(2) Divide the 20-hertz-broadband spectra into frequency bands corresponding to 1/3-octave bands.

(3) Read the broadband sound pressure levels at the center frequencies of the bands.

(4) Convert the 20-hertz-bandwidth levels to 1/3-octave-band levels.

(5) Calculate the discrete-tone levels from 20-hertz-bandwidth spectra.

(6) Obtain the multiple-tone level by logarithmically subtracting the broadband and discrete-tone levels from the known overall 1/3-octave-band levels.

Sample calculations are listed in table I to provide further explanation of the procedure. The example shown in figures 3(a) and (b) is used for the calculations. The results represent test-day data with atmospheric attenuation for one sample run at 90 percent design speed and a 40° azimuth angle. This procedure was applied also for two other sample runs over 1/3-octave bands of interest (with center frequencies from 400 to 8000 Hz) at both speeds considered (60 and 90 percent) and the forward-quadrant azimuth angles at which the data were taken (from 10° to 90° at 10° increments).

Four types of sound pressure levels are listed in table I: band, combined, overall, and total. They are, for the purpose of this report, arbitrarily designated as such to distinguish various levels. When the band levels of any two noise components or several band levels of the same component are logarithmically added, the resulting levels are called combined levels (e.g., the tenth column). When the band levels of all three components are added, the decibel sum is called the overall level (as in the sixth column). The decibel sum over all frequency bands of interest (with center frequencies from 400 to 8000 Hz) is called the total level for any given azimuth angle.

DISCUSSION OF COMPONENT CHARACTERISTICS

The relative significance of the individual noise components is shown in figure 5 for 60 and 90 percent design speed. The figure compares the angular distribution of total, broadband, discrete-tone, and multiple-tone 1/3-octave-band average referred pressure levels of fan B. The figure indicates that at the lower speed the discrete tones have a relatively small effect on the total level, which is approximately equally divided between the broadband noise and multiple-tone noise. To indicate the relative contribution of the broadband noise to the total level, the discrete- and multiple-tone levels are also combined in a single curve. As the fan rotational speed is increased, the contribution of the broadband noise to the total level becomes less important except for the last three angles. However, the contribution of multiple tones for the rest of the angles still remains significant. Except for the first and last two angles, the discrete tones are the dominant noise source for the rest of the azimuth angles.

Multiple Tones

Historically, the multiple tones in the far field were first associated only with fans which had supersonic circumferential rotor tip speeds. This phenomenon was related to the occurrence of leading edge shocks (e.g., refs. 17 to 23). The reason for the circumferential Mach number dependence was that, although the Mach number of the flow relative to the blades at the rotor tip (and not the rotor tip circumferential Mach number) is important for the generation process of the shocks, a ducted pressure field attached to and rotating with a subsonic circumferential tip speed rotor cannot of itself propagate through the fan inlet duct and produce an acoustic pressure field outside the duct (ref. 24). Conversely, a ducted pressure pattern can propagate only if it rotates at supersonic circumferential speed, which in turn depends on the rotor circumferential speed regardless of the generation process. Otherwise, the pressure pattern decays exponentially within the duct before reaching the open end.

Figure 6 shows the variation of sound pressure level of multiple tones on a 2-hertz-bandwidth spectrum for 60, 70, 80, and 90 percent design speed for the frequency range from 0 to 1000 hertz at a 40° front arc azimuth angle. Figure 6 is noteworthy because it shows that for fan B the multiple tones can be easily identified in the far-field spectra of the front quadrant at a majority of shaft-order frequencies at all four subsonic circumferential tip speeds. The circumferential tip Mach numbers corresponding to these speeds ranged from approximately 0.65 to 0.95. The aerodynamic in-duct measurements of fan B (ref. 7) in this Mach number range indicated the existence at the blade tips of pressure patterns resembling leading edge shocks.

Figure 7 further demonstrates the multiple tones on 10-hertz-bandwidth spectra at a 130° rear arc azimuth angle at 60 and 90 percent design speed. Figure 7 shows that the multiple tones can also be identified in the rear quadrant spectra, where the mechanism of rotor leading edge shocks does not apply. However, since the testing was done in an uncontrolled outdoor environment, there is no way of telling whether and how much of this rear quadrant noise was affected by the sound waves radiated from the inlet directly into rear quadrant space. The figure also shows that the multiple tones in the rear quadrant have relatively small pressure levels at either speed, in contrast to the multiple tones in the front quadrant

The appearance of the multiple tones in the front as well as in the rear quadrant spectra is not a unique phenomena of fan B. Recently there have been a number of articles published that show evidence of shaft-order tones generated by fans at subsonic tip speeds (e.g., refs. 24 to 28). Similarly, the phenomenon of the sidebands of these shaft-order tones has also been known for some time (e.g., refs. 29 to 33).

Nevertheless, more information is required about multiple-tone generation at the fan subsonic tip speeds, duct propagation, and radiation into the far field. In particular, more research is required on the multiple-tone clustering phenomena and the relation of the clusters to the discrete-tone skirts and the broadband-noise levels inside the tone skirts. Otherwise, there seems to be general agreement that multiple-tone appearance in far-field spectra, regardless of rotor tip speed, can be linked to blade manufacturing deviations such as blade spacing, stagger angle, twist, thickness, length, camber, and tip clearance. These variations may create a nonuniform acoustic pressure field around the blades which repeats only once per rotor revolution. An additional necessary condition for subsonic tip speed rotors to produce acoustic energy in the far field is the requirement that the pressure fields attached to the rotor blades have to interact either with a stator or with some other circumferential duct or flow irregularity (e.g., ref. 34).

Broadband Noise

Figure 6 illustrates the angular distribution of the broadband levels for 60 and 90 percent design speed. Actual band levels are shown for the bandwidths with center frequencies of the four blade passing frequency harmonics as well as of the two terminal frequencies at 400 and 8000 hertz (added to the figure for comparison). Total actual level (from 20-Hz spectra) and total apparent level (obtained from 1/3-octave-band spectra without a reference to the narrow-band analysis) are also shown.

Comparison of the total apparent and actual broadband levels in figures 8(a) and (b) indicates that, in general, the apparent broadband level is greater than the actual level because the 1/3-octave-band spectral analysis was not capable of distinguishing

multiple-tone content. The degree of the overrating depends on the fan speed. There is relatively good agreement between the actual and apparent broadband levels at the lower (60 percent design) speed. When the fan rotational speed increases, the difference between the two values of broadband-noise levels also increases.

An identical observation was reported by Mugridge and Morfey in reference 26, where a 1/3-octave-band analysis of a single-row low-tip-speed free-vortex type fan spectrum indicated a broadband level 10 decibels higher than actually existed. For this reason, the authors of reference 26 questioned the accuracy of an earlier study by Smith and House (ref. 9) in deriving broadband-noise prediction formulas based on 1/3-octave-band analysis alone.

Comparison of figures 8(a) and (b) also shows that the pressure level of the broadband noise is highly dependent on azimuth angle and speed. At the 60 percent speed, there is a difference between the maximum and minimum total broadband-noise levels of approximately 9 decibels. At 90 percent speed, the broadband-noise level is relatively independent of the azimuth angle. The angular distribution of the broadband noise at arbitrarily selected frequencies indicates that the directionality of the total-broadband-noise levels appears to be affected most by the high-frequency broadband noise (above 4000 Hz for both speeds). Similar variations of broadband sound pressure level with azimuth angles and speeds were observed in the investigations of references 12 and 13.

Further insight into the broadband-noise dependency on azimuth angle and speed, as well as on frequency, is given in figure 9 for 60 and 90 percent design speed. At the lower speed (60 percent), the broadband-noise spectrum levels separate into two distinct groups, depending on the azimuth angle. For angles between 10° and 50°, the spectrum levels indicate a relatively small dependence on the frequency with a slight hump at approximately 4 kilohertz. On the other hand, the arithmetic mean spectrum level at angles between 60° and 90° decreases as frequency increases at a rate of approximately 7 decibels per decade and passes through a 3-decibel-high hump above the mean level (also at 4 kHz). Conversely, at 90 percent speed all azimuth angles appear to correlate about one arithmetic mean level that decreases with increasing frequency at an average rate of approximately 6 decibels per decade.

Distinct broadband-noise humps in the high-frequency region were also observed in the studies of references 35 and 36, which showed that these humps tended to disappear at higher speeds. Similar observations were made in the study of reference 37, where the low-frequency part of the broadband noise was attributed to inflow turbulence which did not affect the high-frequency noise. In contrast, the high-frequency humps were explained as resulting from sources at the fan tips. Clipping away part of the outer trailing edges of the blades reduced the high-frequency humps by over 10 decibels. For the rest of the broadband spectrum, there seems to be a general understanding that

the principal sources of the broadband noise are the nonperiodic random fluctuations of fan blade forces (e.g., refs. 26 and 38 to 41).

Discrete Tones

As discussed in the section Fan Design Characteristics, one of the low-noise features of fan B was its vane-blade number ratio. According to theory (e.g., ref. 34), vane-blade number ratios greater than 2 should assure reduction of the fundamental tone because of the cutoff phenomenon. However, the previously discussed spectra (fig. 3) show prominent blade passing frequency tones for 90 percent speed and a 40° azimuth angle. Figure 10 shows that the fan exhibits significant blade passing frequency tones which dominate the harmonic tones at all forward-quadrant azimuth angles at 60 and 90 percent design speed.

Figure 10 also indicates that, like the apparent broadband noise, the apparent discrete-tone levels (from 1/3-octave-band spectra) exceed the actual tone levels (determined from the 20-Hz narrow-band spectra). The overrating of the apparent discrete-tone levels occurs because of the presence of the multiple tones in the clusters and skirts not only in the parent bands, but also in the adjacent bands, due to the band splitting of the discrete tones on the 1/3-octave-band spectra at both speeds.

Prominent blade passing frequency tones in the inlet far-field spectra have been reported for other fans tested at subsonic tip speeds in the same test site as fan B (e.g., ref. 42). Many of the agents that produce blade passing frequency tones, such as inlet flow distortion, have been traced, at least in part, to the flow obstructions of the test site. For other cases (e.g., ref. 29), theories have now been advanced that relate the appearance of the fundamental tones to inlet flow distortions, inlet turbulence, duct irregularities, crosswinds, irregularities in the boundary-layer thickness, and blade vibration.

CONCLUDING REMARKS

Qualitative and quantitative component and source analyses were performed on arbitrarily selected examples from the acoustic measurements of a transonic fan (fan B of the Quiet Engine Program). The appearance of discrete-tone skirts, multiple-tone clusters, and sidebands on high-resolution narrow-band spectra during the qualitative portion of the component analysis indicated the inadequacy of 1/3-octave-band data (which did not show these components) as a sole source in establishing the proper component levels. It was also indicated that more information is required on the

multiple-tone clustering and coupling phenomena forming the discrete-tone skirts so that the broadband substrata underneath these skirts can be more accurately determined.

The quantitative evaluation of the sound pressure levels of broadband noise, multiple tones, and discrete tones was accomplished from narrow-band spectra in conjunction with 1/3-octave-band spectra. The results showed that the discrete tones and the broadband-noise levels are not as large as they may appear from evaluation of the 1/3-octave-band spectra.

The evaluation of the fan noise spectral components also made it clear that there is a need to replace the long-hand procedure for narrow-band spectra analysis with a programmed procedure which can be adapted to machine calculations. A significant unresolved question is how to program a subjective judgement, which is frequently required in the analysis.

Lewis Research Center,
National Aeronautics and Space Administration,
Cleveland, Ohio, July 9, 1974,
501-04.

APPENDIX - FACILITY AND INSTRUMENTATION

The full-scale-fan acoustic test facility (fig. 1) is located in the open area adjacent to the 10- by 10-Foot Supersonic Wind Tunnel Main Compressor and Drive Building at the NASA Lewis Research Center. The acoustic measurement errors which may be caused by the sound reflection from the building walls are reduced by an acoustic damping material consisting of an open-cell polyurethane ether foam applied to the wall facing the fan. The damping material has relatively good sound absorption properties.

The test fan was located on a concrete foundation about 33.5 meters from the wall and 5.8 meters above the ground level. The fan was positioned to exhaust away from the building. The test fan was driven by the supersonic wind tunnel main drive motors through a speed increasing gearbox, a reversing gearbox, and a series of drive shaft extensions. A semiautomatic speed control held the fan speed to within 3 to 5 rpm of the set speed. The gearboxes and the drive shaft bearing struts were supported by a concrete "viaduct" extending from the building wall to a short distance from the foundation.

In this outdoor environment, far-field acoustic measurements were made by using 16 microphones mounted on the poles at the elevation of the fan axis (fig. 1). All microphones were on 30.5-meter radii in the same horizontal plane with the origin near the exhaust of the fan bypass nozzle.

The condenser microphones used for the measurements had 1.3-centimeter diameters. The microphones were omnidirectional to give a normal incidence free field frequency response which was flat within 1 decibel over 20 to 20 000 hertz. The sensitivity of the microphones was -60 decibels relative to 1 volt per 10^{-1} newton per square meter (1 V/μbar). A 124-decibel, 250-hertz piston phone was used for calibration.

All microphones were equipped with preamplifiers located close to the microphone cartridge for driving the signal over a 152-meter-long cable back to the control room. The control room, located in the main drive building, housed all instrumentation equipment for the test facility. Microphone amplifiers were used for signal conditioning and also for signal monitoring. They also furnished polarization and microphone preamplifier voltage.

All microphone signals were recorded on two 14-channel FM magnetic tape recorders at a tape speed of 152 centimeters per second with a 108-kilohertz center frequency. The individual settings of amplifier gain or attenuation needed to increase or reduce the signal to the amplifier nominal output voltage were manually recorded for each channel. The data reduction equipment consisted of an instrument system that automatically converted the microphone signals to the sound pressure levels. The instrument scanned the incoming signals, passed them one at a time into parallel 1/3-octave-band filters, and then converted the filtered signals into digital voltages

proportional to the root-mean-square values. The recorded level of each filter was the average of a 4-second sample.

Although the fan was also instrumented for aerodynamic testing, no aerodynamic data were used for the present study. The aerodynamic rakes at all stations were removed during the acoustic data acquisition.

REFERENCES

1. Aircraft Engine Noise Reduction. NASA SP-311, 1972.

2. Montegani, Francis J.: Noise Generated by Quiet Engine Fans. I - Fan B. NASA TM X-2528, 1972.

3. Kramer, J. J.; and Montegani, F. J.: The NASA Quiet Engine Program. Paper 72-GT-96, ASME, Mar. 1972.

4. Montegani, Francis J.: Some Propulsion System Noise Data Handling Conventions and Computer Programs Used at the Lewis Research Center. NASA TM X-3013, 1974.

5. Leonard, Bruce R.; Schmiedlin, Ralph F.; Stakolich, Edward G.; and Neumann, Harvey F.: Acoustic and Aerodynamic Performance of a 6-Foot-Diameter Fan for Turbofan Engines. I - Design of Facility and QF-1 Fan. NASA TN D-5877, 1970.

6. Experimental Quiet Engine Program. Vol. 1. Phase I: Engine Design Report. General Electric Co. (NASA CR-72967), 1970.

7. Giffin, R. G.; Parker, D. E.; and Dunbar, L. W.: Experimental Quiet Engine Program, Aerodynamic Performance of Fan B. General Electric Co. (NASA CR-72993), 1972.

8. Sharland, I. J.: Sources of Noise in Axial Flow Fans. J. Sound Vib., vol. 1, no. 3, 196[illegible], pp. 302-322.

9. Smith, M. J. T.; and House, M. E.: Internally Generated Noise From Gas Turbine Engines. Measurement and Prediction. Paper 66 - GT/N-43, ASME, Mar. 1966.

10. Richards, Elfyn J.; and Mead, D. J.; eds.: Noise and Acoustic Fatigue in Aeronautics. John Wiley & Sons, 1968.

11. Goldstein, Arthur W.; Lucas, James G.; and Balombin, Joseph R.: Acoustic and Aerodynamic Performance of a 6-Foot-Diameter Fan for Turbofan Engines. II - Performance of QF-1 Fan in Nacelle Without Acoustic Suppression. NASA TN D-6080, 1970.

12. Benzakein, M. J.; Hochheiser, R. M.; Claes, H. P.; Kasin, S. B.; and Conrad, W. E.: Fan/Compressor Noise Research. General Electric Co. (FAA-RD-71-85-vol. 2; AD-740515), 1971.

13. Burdsall, E. A.; and Urban, R. H.: Fan-Compressor Noise: Prediction, Research, and Reduction Studies. Pratt & Whitney Aircraft (FAA-RD-71-73), 1971.

14. Beranek, Leo L., ed.: Noise Reduction. McGraw-Hill Book Co., 1960.

15. Harris, Cyril M., ed.: Handbook of Noise Control. McGraw-Hill Book Co., 1957.

16. Bickel, Henry J.: Calibrated Frequency-Domain Measurements, Using the Ubiquitous Spectrum Analyzer. Monagraph No. 2, FSC-M-71/100B, Federal Scientific Corp., 1969.

17. Hawkings, D.: Multiple Tone Generation by Transonic Compressors. J. Sound Vib., vol. 17, no. 2, Jul. 1971, pp. 241-250.

18. Kurosaka, M.: A Note on Multiple Pure Tone Noise. J. Sound Vib., vol. 19, no. 4, Dec. 1971, pp. 453-462.

19. Kester, J. D.; and Pickett, G. F.: Application of Theoretical Acoustics to the Reduction of Jet Engine Noise. J. Phys. D. Appl. Phys. vol. 5, Jan. 1972, pp. 12-27.

20. Pickett, Gordon F.: Prediction of the Spectral Content of Combination Tone Noise. J. Aircraft, vol. 9, no. 9, Sept. 1972, pp. 658-663.

21. Sofrin, T. G.: Fan Noise Mechanism and Control. I. In Inter-Noise 72; International Conference on Noise Control Engineering, Washington, D. C., Oct. 4-6, 1972, pp. 458-466.

22. Kantola, R. A.; and Kurosaka, M.: Theoretical and Experimental Investigation on Multiple Pure Tone Noise. J. Aircraft, vol. 9, no. 11, Nov. 1972, pp. 784-790.

23. McCune, James E.; and Kerrebrock, Jack L.: Noise From Aircraft Turbomachinery. In: Annual Review of Fluid Mechanics, vol. 15, Annual Reviews, Inc., Palo Alto, Calif., 1973, pp. 281-300.

24. Mather, J. S. B.; Savidge, J.; and Fisher, M. J.: New Observation on Tone Generation in Fans. J. Sound Vib., vol. 16, no. 3, June 1971, pp. 407-418.

25. Barry, B.; and Moore, C. J.: Subsonic Fan Noise. J. Sound Vib., vol. 17, no. 2, Jul. 1971, pp. 207-220.

26. Mugridge, B. D.; and Morfey, C. L.: Sources of Noise in Axial Flow Fans. J. Acoust. Soc. Amer., vol. 51, no. 5 (pt. 1), 1972, pp. 1411-1426.

27. Moore, C. J.: In-Duct Investigation of Subsonic Fan "Rotor Alone" Noise. J. Acoust. Soc. Amer., vol. 51, no. 5 (pt. 1), 1972, pp. 1471-1482.

28. Krishnappa, G.: Lifting Fan Noise Studies With Superimposed Cross Flows. J. Aircraft, vol. 9, no. 10, Oct. 1972, pp. 719-725.

29. Benzakein, M. J.: Research on Fan Noise Generation, J. Acous. Soc. Amer., vol. 51, no. 5 (pt. 1), 1972, pp. 1427-1438.

30. Taylor, Ralph E., ed.: Radio Frequency Interference Handbook. NASA SP-3067, 1971.

31. Griffiths, J. W. R.: The Spectrum of Compressor Noise of a Jet Engine. J. Sound Vib., vol. 1, no. 2, 1964, pp. 127-140.

32. MacFarlane, G. G.: On the Energy-Spectrum of an Almost Periodic Succession of Pulses. IRE Proc., vol. 37, no. 10, Oct. 1949, pp. 1139-1143.

33. Lowson, M. V.: Rotor Noise Radiation in Nonuniform Flow. In: Loughborough University of Technology, Symposium on Aerodynamic Noise, Loughborough, Leics., England, September 14-17, 1970, pp. D.2.1-D.2.20.

34. Tyler, J. M.; and Sofrin, T. G.: Axial Flow Compressor Noise Studies. S.A.E. Trans., vol. 70, 1962, pp. 309-332.

35. Leverton, J. W.: The Noise Characteristics of a Large "Clean" Rotor. J. Sound Vib., vol. 27, no. 3, Apr. 1973, pp. 357-376.

36. Laverton, J. W.; and Pollard, J. S.: A Comparison of the Overall and Broadband Noise Characteristics of Full-Scale and Model Helicopter Rotors. J. Sound Vib., vol. 30, no. 2, Sept. 1973, pp. 135-152.

37. Lowson, M. V.; Whatmore, A. R.; and Whitfield, C. E.: Studies of Noise Radiation by Rotating Blades. Interagency Symposium on University Research in Transportion Noise, Book of Proceedings, vol. 1, Stanford, Calif., Mar. 28-30, 1973, pp. 211-224.

38. Morfey, C. L.; and Tanna, H. K.: Sound Radiation From a Point Force in Circular Motion. J. Sound Vib., vol. 1 , no. 3, Apr. 1971, pp. 325-352.

39. Tanna, H. K.; and Morfey, C. L.: Sound Radiation From Point Sources in Circular Motion. J. Sound Vib., vol. 16, no. 3, June 1971, pp. 337-348.

40. Tanna, H. K.: Sound Radiation From Point Acoustic Stresses in Circular Motion. J. Sound Vib., vol. 16, no. 3, June 1971, pp. 349-364.

41. Chandrashekhara, N.: Sound Radiation From Inflow Turbulence in Axial Flow Fans. J. Sound Vib., vol. 19, no. 2, Nov. 1971, pp. 133-146.

42. Povinelli, Frederick P.; Dittmar, James H.; and Woodward, Richard P.: Effect of Installation Caused Flow Distortion on Noise From a Fan Designed for Turbofan Engines. NASA TN D-7076, 1972.

TABLE I. - SAMPLE CALCULATIONS OF NOISE COMPONENT SOUND PRESSURE LEVELS OF ONE TEST-DAY RUN

[90 Percent design speed, 40° azimuth angle.]

1/3-Octave-band analysis						Actual broadband level		Actual discrete-tone level		Multiple-tone level, dB[a]
Band	Lower frequency, Hz	Center frequency, Hz	Upper frequency, Hz	Bandwidth, Hz	Overall level, dB[a]	20-Hz spectra, dB[a]	1/3-Octave-band spectra, dB[a]	20-Hz spectra, dB[a]	1/3-Octave-band spectra combined with broadband level, dB[a]	
10	355	400	447	92	87.5	83.0	87.5	-----	87.5	[b]75.0
11	447	500	563	116	88.0	82.5	88.0	-----	88.0	[b]75.5
12	563	630	709	146	89.0	82.0	88.5	-----	88.5	79.5
13	709	800	892	183	91.0	81.0	88.5	-----	88.5	87.5
14	892	1000	1120	228	91.0	80.5	89.0	-----	89.0	86.5
15	1120	1250	1410	290	107.5	80.0	89.5	108.5	108.5	------
					[c]109.5		[c]93.0		[c]108.5	[c]102.5
16	1410	1600	1780	370	105.5	80.0	90.5	-----	90.5	------
17	1780	2000	2240	460	94.0	79.5	91.0	-----	91.0	91.0
18	2240	2500	2820	580	102.0	79.0	91.5	102.0	102.5	------
					[c]104.5		[c]95.0		[c]103.0	[c]99.0
19	2820	3150	3550	730	101.0	78.5	92.0	-----	92.0	------
20	3550	4000	4470	920	99.5	78.0	92.5	95.5	97.5	95.0
21	4470	5000	5630	1160	96.0	78.0	93.5	89.5	95.0	89.0
22	5630	6300	7090	1460	95.0	77.5	94.0	85.5	94.5	85.5
23	7090	8000	8920	1830	93	75.5	93.0	81.5	93.0	80.5
Total level	----	----	----	----	111.5	----	102.5	109.5	------	105.0

[a]Re. 2×10^{-5} N/m^2 (2×10^{-4} μbar).

[b]Estimated maximum probable levels (±0.2 dB).

[c]Combined band level due to band splitting.

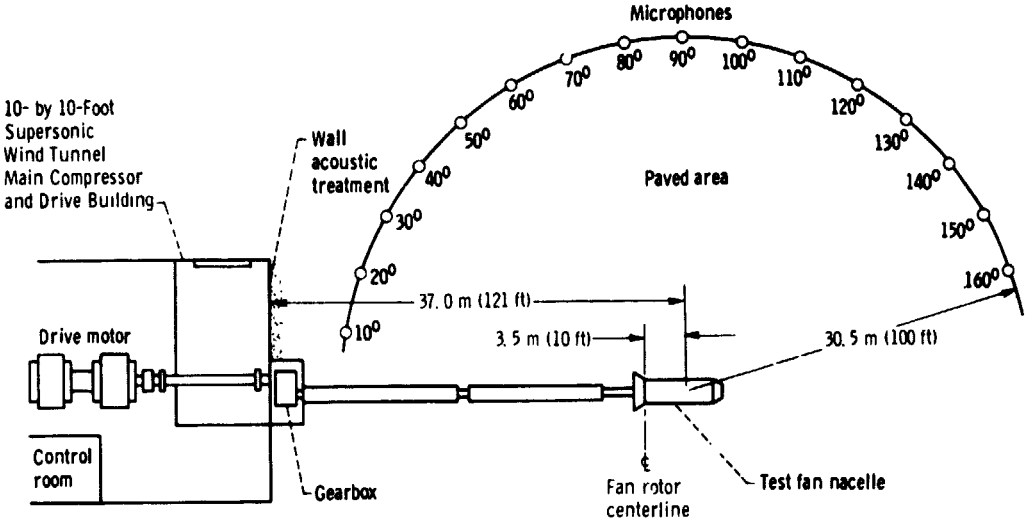

Figure 1. - Plan view of full-scale-fan acoustic test facility.

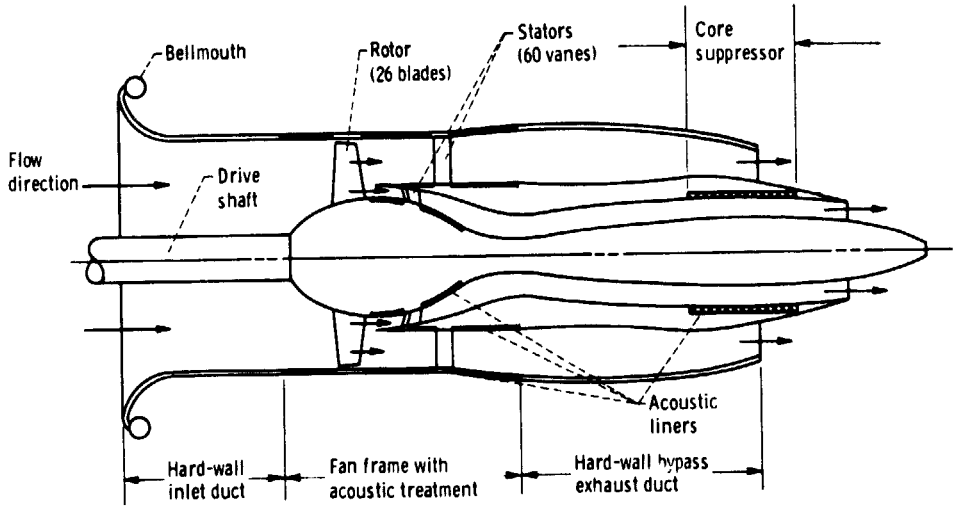

Figure 2. - Arrangement of flow passages and design features of fan B configuration.

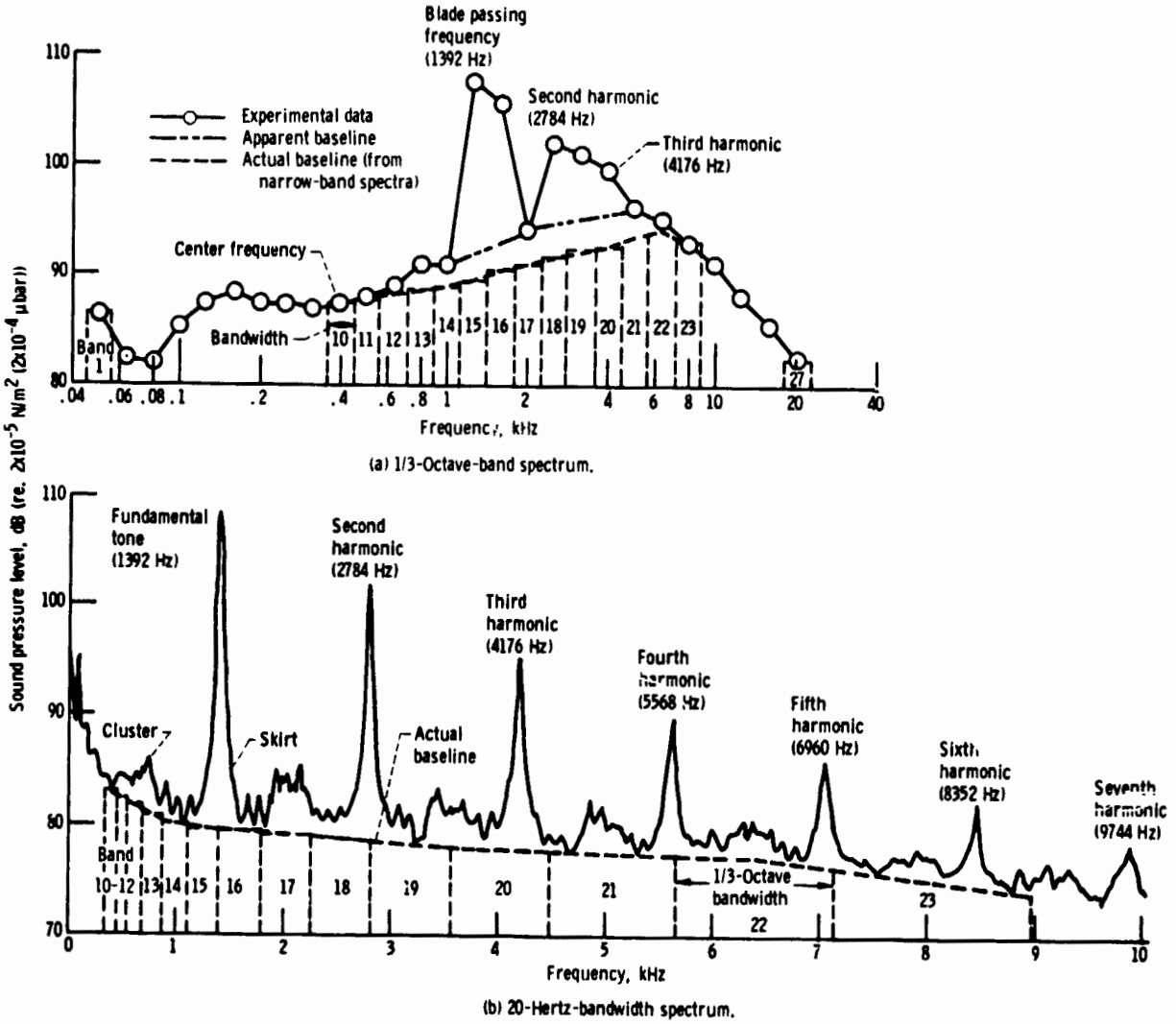

(a) 1/3-Octave-band spectrum.

(b) 20-Hertz-bandwidth spectrum.

Figure 3. - Spectral distribution of test-day sound pressure level of sample run at 40° azimuth angle at 90 percent design speed.

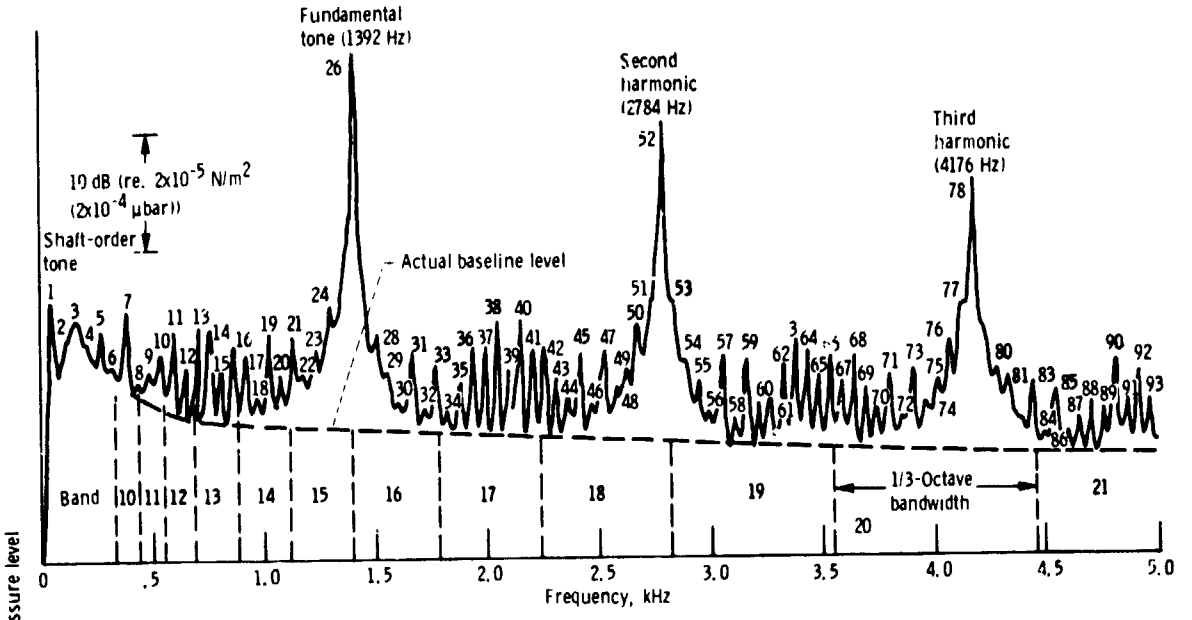

(c) 10-Hertz-bandwidth spectrum.

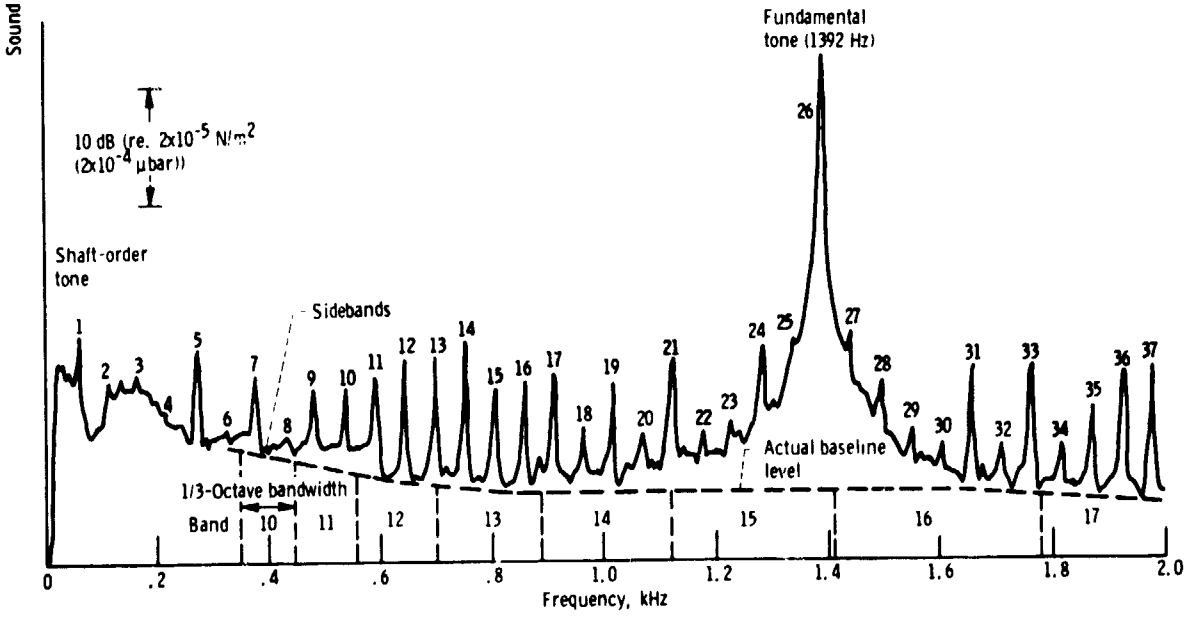

(d) 4-Hertz-bandwidth spectrum.

Figure 3. - Concluded.

(a) Multiple tones as combination of shaft-order tones and sidebands in a cluster.

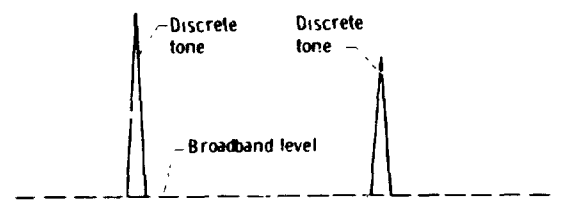

(b) Discrete tones superimposed on broadband base.

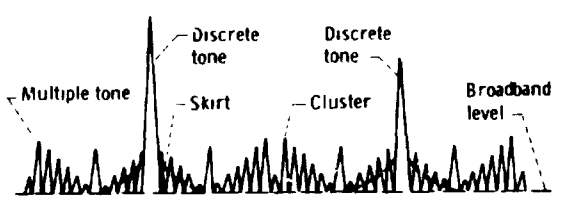

(c) Complete spectrum of discrete tones, multiple tones, and sidebands superimposed on broadband-noise baseline and forming clusters and skirts.

Figure 4. - Basic spectral features of fan B noise.

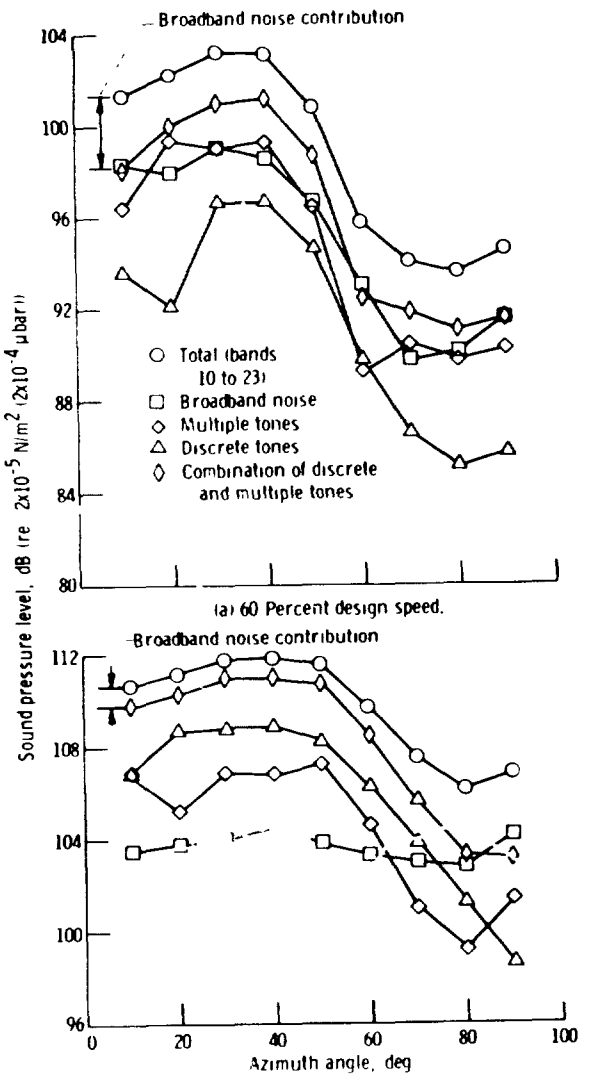

(a) 60 Percent design speed.

(b) 90 Percent design speed.

Figure 5 - Angular distribution of referred pressure levels of noise components.

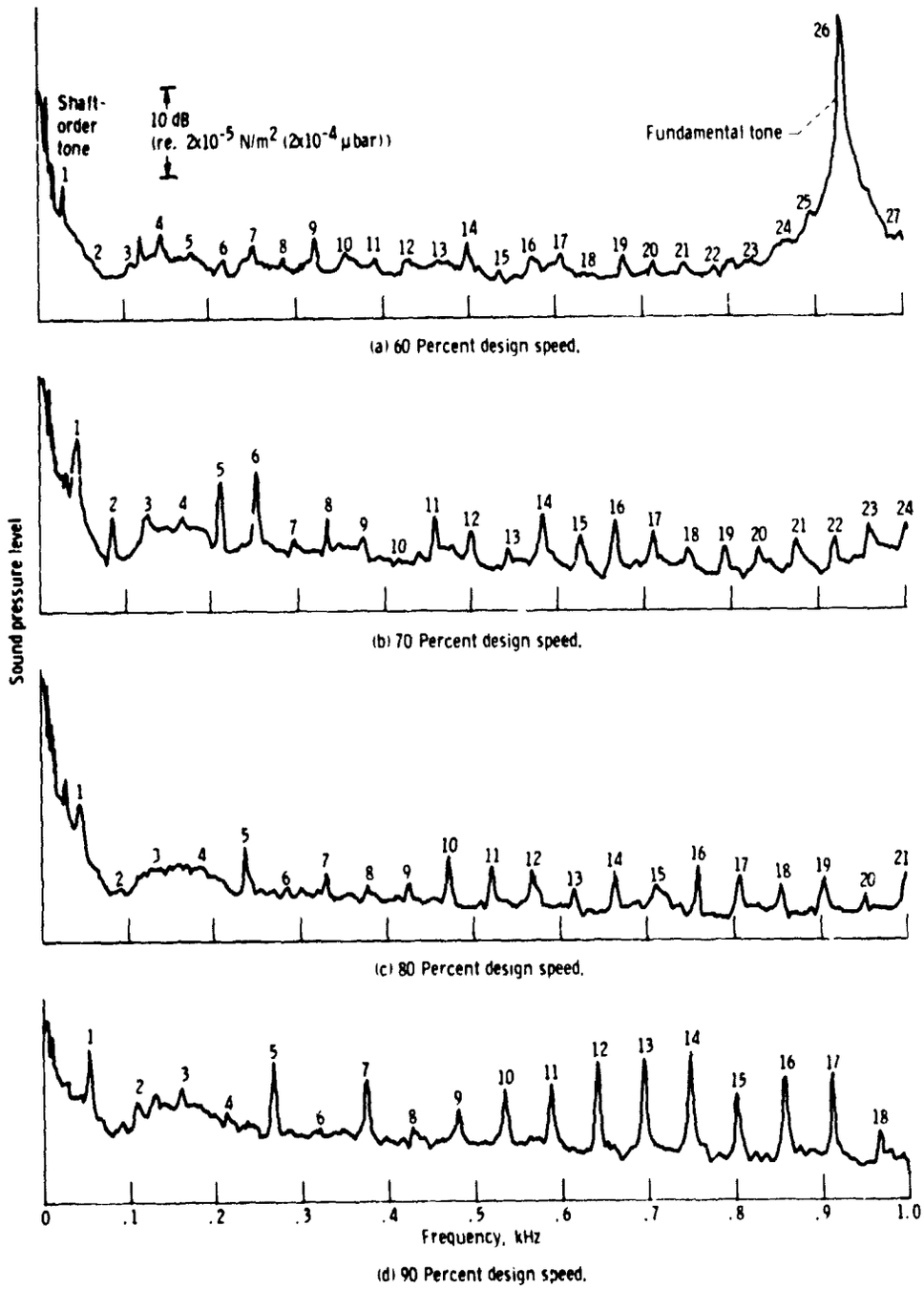

(a) 60 Percent design speed.

(b) 70 Percent design speed.

(c) 80 Percent design speed.

(d) 90 Percent design speed.

Figure 6. - Variation of multiple tones with fan speed and frequency on 2-hertz-bandwidth spectrum at 40° azimuth angle (forward quadrant).

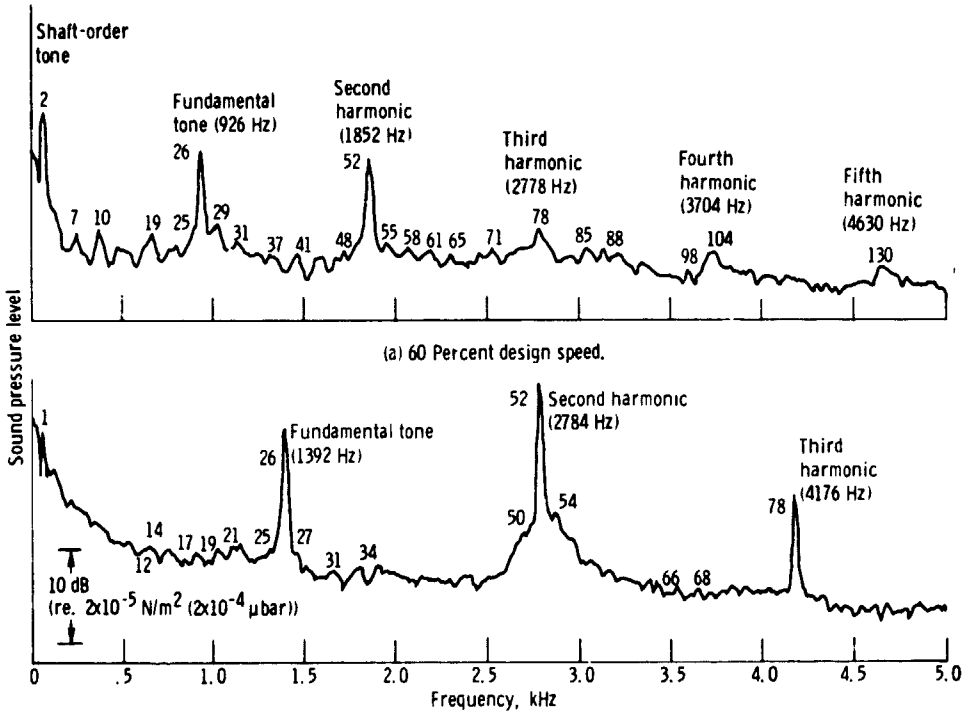

Figure 7. - Variation of multiple tones with fan speed and frequency on 10-hertz bandwidth spectrum at 130° azimuth angle (rear quadrant).

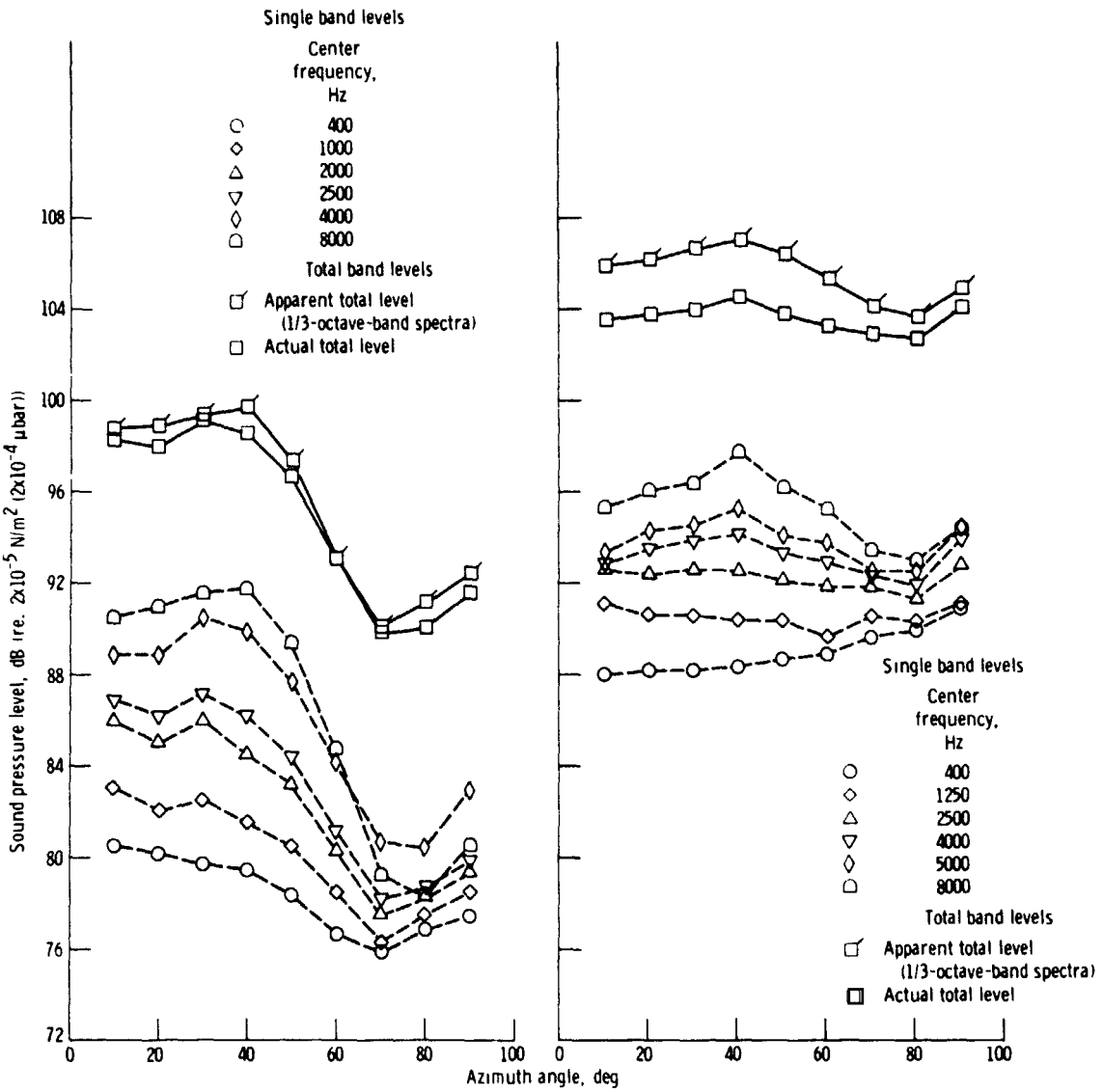

(a) 60 Percent design speed.

(b) 90 Percent design speed.

Figure 8. - Angular distribution of referred pressure levels of broadband noise.

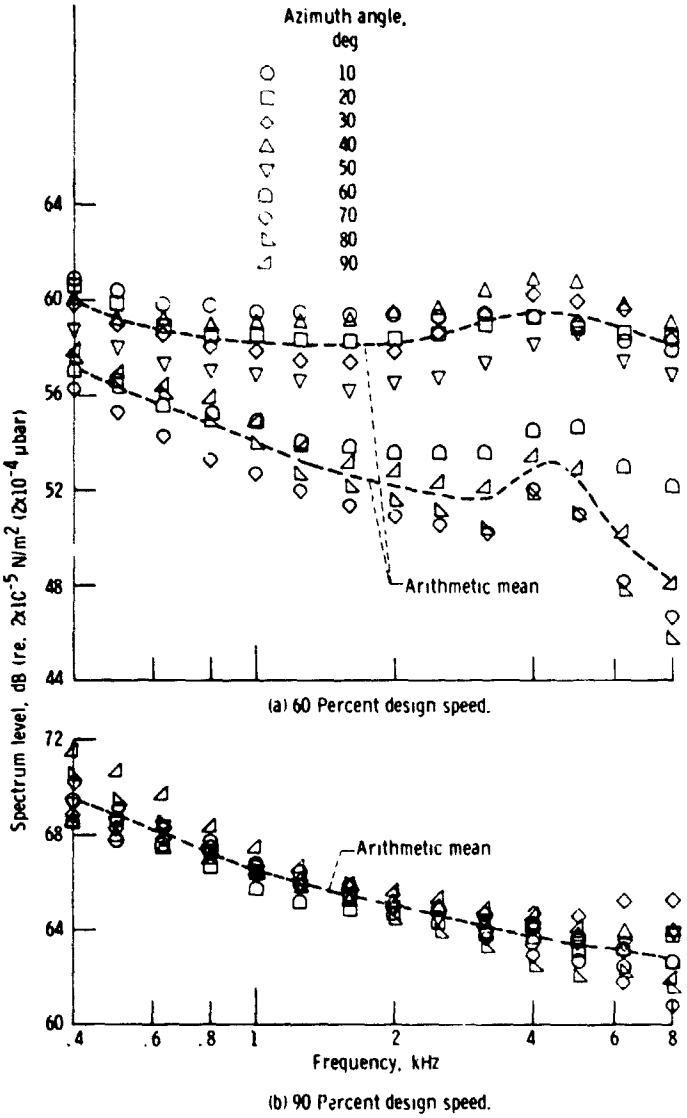

Figure 9. - Variation of broadband spectrum level with angle.

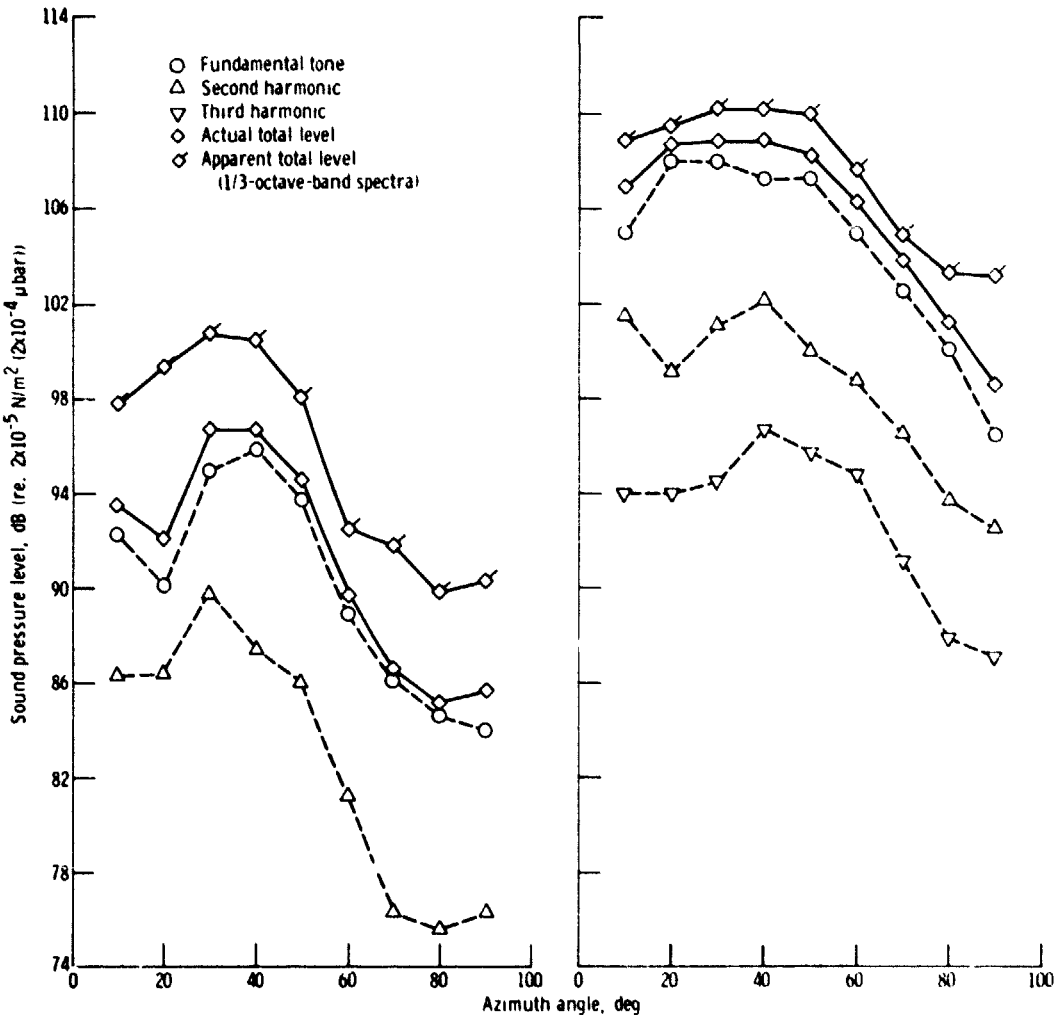

(a) 60 Percent design speed.

(b) 90 Percent design speed

Figure 10. - Angular distribution of referred pressure level of discrete tones.

NASA-Langley, 1974 E-7989